Received: 11 May 2021 | Revised: 6 September 2021 | Accepted: 9 September 2021

DOI: 10.1096/fj.202100778RRRR

THE FASEB JOURNAL

RESEARCH ARTICLE

A recombinant glucocorticoid-induced leucine zipper protein ameliorates symptoms of dextran sulfate sodium-induced colitis by improving intestinal permeability

Marco Gentili[1] | **Laura Hidalgo-Garcia**[2,3] | **Teresa Vezza**[2,3] | **Erika Ricci**[1] | **Graziella Migliorati**[1] | **Alba Rodriguez-Nogales**[2,3] | **Carlo Riccardi**[1] | **Julio Galvez**[2,3] | **Simona Ronchetti**[1]

[1]Pharmacology Division, Department of Medicine and Surgery, University of Perugia, Perugia, Italy

[2]CIBER-EHD, Department of Pharmacology, ibs.GRANADA, Center for Biomedical Research (CIBM), University of Granada, Granada, Spain

[3]Instituto de Investigación Biosanitaria de Granada (ibs.GRANADA), Granada, Spain

Correspondence
Simona Ronchetti, Pharmacology Division, Department of Medicine and Surgery, University of Perugia, Perugia 06132, Italy.
Email: simona.ronchetti@unipg.it

Funding information
Italian Ministry of Education, Universities and Research, Grant/Award Number: PRIN 2017B9NCSX; Vini di Batasiolo S.p.A.; Junta de Andalucia, Grant/Award Number: CTS 164; Instituto de Salud Carlos III, Grant/Award Number: PI19/1058 and CP19/00191; EMBO

Abstract

Inflammatory bowel diseases (IBDs) are chronic inflammatory disorders characterized by relapsing intestinal inflammation, but many details of pathogenesis remain to be fully unraveled. Glucocorticoid (GC)-induced leucine zipper (GILZ) is a mediator of the anti-inflammatory effects of GCs, the most powerful drugs for IBD treatment, but they cause several unwanted side effects. The fusion protein TAT-GILZ has been successfully used in some pre-clinical models of inflammatory and autoimmune diseases. To test the efficacy of TAT-GILZ for treating dextran sulfate sodium (DSS)-induced colitis and explore its impact on the gut microbiome, colitis was induced by DSS in C57BL/6J mice and treated with TAT-GILZ or dexamethasone. Various hallmarks of colitis were analyzed, including disease activity index, gut permeability, and expression of pro-inflammatory cytokines and tight junction proteins. TAT-GILZ treatment showed a therapeutic effect when administered after the onset of colitis. Its efficacy was associated with improved gut permeability, as evidenced by zonula occludens-1 and CD74 upregulation in inflamed colonic tissue. TAT-GILZ also ameliorated the changes in the gut microbiota induced by the DSS, thus potentially providing an optimal environment for colonization of the mucosa surface by beneficial bacteria. Overall, our results demonstrated for the first time that TAT-GILZ treatment proved effective after disease onset allowing restoration of gut permeability, a key pathogenic feature of colitis. Additionally, TAT-GILZ restored gut dysbiosis, thereby

Abbreviations: AMPs, antimicrobial proteins; CD, Crohn's disease; DAB, diaminobenzidine; DAI, disease activity index; DEX, dexamethasone; DNBS, dinitrobenzene sulfonic acid; DSS, dextran sulfate sodium; EAE, experimental autoimmune encephalomyelitis; GC, glucocorticoids; GILZ, glucocorticoid leucine zipper gene; IBD, inflammatory bowel disease; KO, knock-out; LPS, lipopolysaccharide; OD, optical density; PCoA, principal coordinate analysis; sIgA, secretory immunoglobulin A; STAMP, statistical analysis of metagenomic profiles; TAT, transactivator of transcription; Th, T helper; UC, ulcerative colitis; WT, wild type; ZO-1, zonula occludens-1.

Julio Galvez and Simona Ronchetti have contributed equally to the supervision of the study.

contributing to healing mechanisms. Interestingly, we found unprecedented effects of exogenous GILZ that did not overlap with those of GCs.

KEYWORDS
colitis, dysbiosis, GILZ, glucocorticoids, microbiota

1 | INTRODUCTION

Inflammatory bowel disease (IBD) encompasses chronic relapsing inflammatory disorders of the gastrointestinal tract, mainly Crohn's disease (CD), and ulcerative colitis (UC), whose pathogenic mechanisms remain poorly understood. IBD is characterized by a disrupted mucosa structure, altered gut microbial composition (dysbiosis), and systemic biochemical abnormalities. There is a need to establish appropriate therapeutic approaches for IBD, and various studies have explored the molecular pathways underlying these conditions. Both CD and UC are considered immune-mediated inflammatory diseases, in which $CD4^+$ T cells play a pivotal role. CD is typically characterized by a prevalent and inflammatory Th1 cell phenotype, whereas UC is associated with a pathogenic Th2 cell phenotype.[1,2] Different drugs are available for IBD treatment, including biologicals, but none can completely cure IBDs.[3–6] Among effective drugs, glucocorticoids (GCs) are the first line of treatment for IBDs, since they can achieve complete remission, albeit with various caveats, including the development of resistance and the occurrence of severe adverse effects. Alternative and efficacious therapies are urgently needed due to the high prevalence among populations all over the world, which is increasing especially in young people.[7]

Glucocorticoid-induced leucine zipper (GILZ, or tsc22d3) is an early-transcribed anti-inflammatory gene induced by glucocorticoid treatment. GILZ mediates glucocorticoid functions without eliciting the adverse effects that are typical of glucocorticoid treatment.[8–10] The use of GILZ-based proteins as pharmacological tools to treat inflammatory or autoimmune diseases has been described in successful pre-clinical studies, including mouse models of Dinitrobenzene sulfonic acid (DNBS)-induced colitis and experimental autoimmune encephalomyelitis (EAE).[5,11–13] A recombinant TAT-GILZ protein reversed the symptoms of DNBS-induced colitis in GILZ B cell-conditional knock-out mice, as well as in wild type (WT) mice.[14] Similarly, administration of TAT-GILZ protein ameliorated colitis in *IL-10*-KO mice, which spontaneously develop this disease.[13] The mechanisms by which GILZ exerts its therapeutic effects are not completely understood, but cells related to innate and adaptive immunity are involved in this process.[15,16]

The aim of the present work was to explore the treatment of dextran sulfate sodium (DSS)-induced colitis with a recombinant TAT-GILZ protein following a curative dosing protocol, in which test compound was administered soon after disease onset. The results revealed that the beneficial effects exerted by the recombinant TAT-GILZ protein were associated with improving intestinal epithelial barrier function and ameliorating colitis-associated dysbiosis, which characterizes intestinal inflammation.

2 | MATERIALS AND METHODS

2.1 | Animals

C57BL/6 male mice weighing 20–25 g, 6- to 8-week old, were purchased from Janvier Labs (Saint Berthevin Cedex, France). All mice were housed under specific pathogen-free conditions and a 12–12-h light/dark cycle, receiving water and food ad libitum, in accordance with the Animals (Scientific Procedures) Act 1986 Amendment Regulations (SI 2012/3039) and the EU Directive 2010/63/EU and in compliance with the ARRIVE guidelines.[17]

2.2 | DSS-induced colitis

All animal studies were carried out in accordance with the 'Guide for the Care and Use of Laboratory Animals' as promulgated by the National Institute of Health. Mice were randomly allocated into five groups with eight mice in each, including one non-colitic and four DSS-treated groups. Colitis was induced by adding 3% DSS (36–55 KDa; MP Biomedicals, Santa Ana, CA, USA) in autoclaved drinking water ad libitum until day 4. From day 4 to day 9 the four colitic groups were treated with dexamethasone (DEX, 1 mg/Kg) (Eurogenerici, Milan, Italy), freshly prepared TAT (0.1 mg/kg) and TAT-GILZ (0.2 mg/kg), a cell-permeable GILZ fusion protein, dissolved in saline solution, or saline solution (200 µl). TAT and TAT-GILZ proteins were produced in a Lipopolysaccharide (LPS)-free system as described previously.[13] TAT-GILZ dosage was chosen according to previously published studies.[18] Two hundred microliter of each treatment were administered intraperitoneally (i.p.) daily. All mice were fed with

standard chow for the whole experiment. The disease activity index (DAI) was evaluated daily for each animal according to the scores listed in Table 1.

DAI value is the combined scores for weight loss, stool consistency, and rectal bleeding divided by 3.

Each mouse weight was registered daily. At day 9, mice were sacrificed and colons removed, emptied, and weighted. The distal part of the colon (rectum) was separated and fixed in 4% formaldehyde for histological studies.

2.3 | In vivo intestinal permeability assay

Mice from each group ($n = 4$) were fasted for 12 h to empty the colon prior to dextran-4000-FITC (350 mg/kg) administration by oral gavage. After four hours, blood samples were collected by cardiac puncture and centrifuged for 10 min at 4°C. Plasma was diluted (1:20) in phosphate-buffered saline (PBS) and the dextran-4000-FITC was measured using Fluorostart fluorescence spectrophotometer (BMG Lab Technologies, Offenburg, Germany) at an excitation wavelength of 485 nm and emission wavelength of 535 nm. Standard curves were obtained by serial dilution of dextran-4000-FITC in PBS.

2.4 | qRT-PCR

Five milligram sample of each colon was used for mRNA extraction with an RNeasy Plus Mini Kit (Qiagen). Conversion of total mRNA to cDNA was performed using a High-Capacity cDNA Reverse Transcription Kit (Qiagen, Hilden, Germany). All real-time PCR steps were performed using the 7300 Real Time PCR System (Applied Biosystem) and cDNA amplified by using TaqMan Gene Expression Master Mix (Applied Biosystem) and cDNA was amplified using TaqMan Gene expression Master Mix (Applied Biosystem). mRNA expression was detected using the probes: CD74, CD44, Tbx21, Gata3, RorC, FoxP3, Il-10, Tgf β, Il-1β, IL-6, and TNF-α, (Thermo Fisher Scientific, Waltham, MA, USA). Normalization was performed using the 18S ribosomal RNA housekeeping gene, and relative expression levels were calculated using the $2^{-\Delta Ct}$ method. SYBR Green Master Mix (Thermo Fisher Scientific) was used to detect cyclins D1, D2 and D3 with the following primers: forward primer 5′ CGTGGCCTCTAAGATGAAGG 3′ and reverse primer 5′ TGAGCTTGTTCACCAGAAGC to amplify cyclin D1; forward primer 5′ GCCAAGATCACCCACACTG 3′ and reverse primer 5′ ATGACGAACACGCCTCTCTC 3′ to amplify cyclin D2; forward primer 5′ CGAGCCTCCTACTTCCAGTG 3′ and reverse primer 5′ AGGCAGACGGTACCTAGAAGC 3′ to amplify cyclin D3.

2.5 | Western blotting

Total colon proteins were extracted using RIPA buffer (10 mM Tris-HCl, pH 8.0, 1 mM EDTA, 1% NP-40, 0.1% SDS, 140 mM NaCl) with inhibitors (PMSF 1:100, protease inhibitor cocktail 1:1000, sodium orthovanadate 1:200, phosphatase inhibitor 1:100). Following protein quantification, 20 μg of protein per sample were subjected to 10% SDS-PAGE. Membranes were blocked for 1 h with TBST with 5% non-fat dried milk (NFDM) and incubated overnight at 4°C with primary antibodies specific to phospho-ERK (9101s, 26), total ERK (#9102s, 26) (Cell Signaling, Leiden, the Netherlands), and lamin-β (#ab16048, GR 3369248-1) (Abcam, Cambridge, UK). After five washes in 1× tris-buffered saline (TBS), 0.1% Tween 20, secondary anti-rabbit antibody labelled with horseradish peroxidase (Pierce, Thermo Fisher Scientific, Waltham, MA, USA) was diluted 1:5000 in 5% NFDM and incubated for 1 h at r.t. Antigen-antibody complexes were detected by enhanced chemiluminescence in accordance with the manufacturer's instructions (Millipore, Billerica, MA, USA). Band signal intensities of western blot films were assessed using ImageJ software. Lamin-β was used as a loading control, and activation of ERK was expressed as a ratio of phosphorylated/total protein levels.

2.6 | Hematoxylin and eosin staining

Sections of colon tissue were fixed in 4% formalin for 24 h, dehydrated using 70%, 80%, 90%, 95%, and 100% ethanol

TABLE 1 Disease activity index (DAI) score used to evaluate DSS-induced colitis

Bleeding	Stool consistency	Weight loss (WL, %)	Value assigned according to WL
0: normal	**0**: normal	0	**0**
1: presence of blood	**1**: moderate soft stools	1–5	**1**
2: moderate bleeding	**2**: soft stools	6–10	**2**
3: moderately high bleeding	**3**: soft stools and diarrhea	11–20	**3**
4: abundant bleeding	**4**: diarrhea	> 20	**4**

Bold values originate the DAI score.

and xylene, and finally embedded in wax blocks. Blocks were cut in 4 μm slices, placed on a glass support, dewaxed, stained with hematoxylin for 5 min, washed with PBS, differentiated in 1% hydrochloric acid alcohol, stained with eosin solution for 30 s, dehydrated in gradient alcohol, and mounted in water-based mountant. Examination of IHC was performed as described previously.[19] Epithelial damage and crypt loss analysis was performed according to standardized criteria as previously described and blinded evaluated.[20]

2.7 | Immunohistochemistry

Paraffin-embedded colons where sliced into 4 μm sections, mounted on polylysined-coated glass, washed twice for 10 min each time in Xilolo to deparaffinize the sections, and rehydrated with decreasing concentrations of ethanol in water. Immunohistochemistry was performed using the diaminobenzidine (DAB) solution method with a 2-step plus Poly-HRP Anti Rabbit IgG Detection System (With DAB Solution) (Elabscience, Houston, TX, USA). Antigen retrieval was achieved by boiling in sodium citrate buffer (pH 6.0) for 1 h, and subsequently cooling for 20 min. Endogenous peroxidases were blocked by incubating 10 min with 3% hydrogen peroxide. Sections were then washed with PBS for 10 min and then incubated for 20 min with blocking buffer (supplied in the kit). Anti-ZO1 (Abcam ab96587, GR 3283386-5, 1:500) was added and incubated overnight at 4°C. Sections were rinsed in PBS (2 × 10 min) and incubated for 45 min at room temperature with biotinylated goat anti-rabbit antibody (supplied in the kit), then washed in PBS for 10 min. Signal detection was performed using 3′-diaminobenzidine and the reaction was stopped with water after microscope observation. Slides were counterstained with Mayer's hematoxylin (BIO-OPTICA, Milan, Italy) and washed in running water. Slides were finally dehydrated in graded ethanol, defatted in xylene and covered with Entellan New Mountant (Merck, Darmstadt, Germany). Stained sections were examined under bright-field illumination on a Nikon Eclipse E800 microscope (Nikon Canada, Mississauga, ON). Digital images were acquired with an Optronics camera using Neurolucida software (Microbrightfield, Winooski, VT, USA) and optical density quantization was performed using ImageJ Fiji software.

2.8 | Microbiota characterization, DNA extraction, and sequencing analysis

Colonic luminal contents were collected from all animals at the endpoint of the experiment and immediately stored at −80°C until DNA extraction. Total DNA was isolated following a procedure described previously.[21] Amplicon fragments were amplified by PCR in duplicate using separate template dilutions (1:10) with high-fidelity Phusion polymerase. A single round of PCR was performed using fusion primers targeting 16S V4-V5 regions via multiplexing on an Illumina MiSeq instrument (Illumina Inc., San Diego, CA, USA). PCR products from the same samples were pooled in one plate, purified and normalized, then pooled to make one library that was quantified fluorometrically before sequencing. In details, the normalization procedure required different steps. Firstly, after DNA sequencing, all reads were scored for quality, and any poor quality and short reads were removed. Then, the resulting sequences were clustered and taxonomically assigned on the basis of 97% similarity level against the Greengenes Database using QIIME software package (Version 1.9.1) (Knight Lab, San Diego, CA, USA). Sequences were selected to estimate the total bacterial diversity of the DNA samples in a comparable manner and were trimmed to remove barcodes, primers, chimeras, plasmids, mitochondrial DNA and any non-16S bacterial reads and sequences <150 bp. Lastly, the normalization procedure was performed by operational taxonomic unit matrices by rarefying, in which the samples with total counts below the threshold were excluded and the rarefaction curves were determined. For microbiota evaluation, the Metagenomic Analysis Server (MG-RAST)[22] and the Greengenes Database were employed. The output file was further analyzed using the SPSS Statistics 17.0 software package (SPSS Inc., Chicago, IL, USA) and the Statistical Analysis of Metagenomic Profiles software package (version 2.1.3).

2.9 | Data and statistical analyses

All data are expressed as mean ± standard error. Differences between mean values were tested for statistical significance using one-way analysis of variance and post-hoc least significance tests. All statistical analysis was performed using GraphPad Prism 6.0 software (*$p < .05$, **$p < .01$, ***$p < .001$, ****$p < .0001$).

3 | RESULTS

3.1 | TAT-GILZ treatment ameliorates colitis symptoms

To investigate the effect of recombinant TAT-GILZ protein in the context of colitis as a potential pharmaceutical tool, we induced DSS-driven colitis in C57Bl/6 mice and included one non-colitic control group. After 4 days

of the disease, at the onset of colitis symptoms, TAT-GILZ, control TAT, glucocorticoid DEX or saline were administered daily for the next 5 days. Daily weight loss percentage and DAI scores for each group are shown in Figure 1A. Interestingly, both weight loss percentage and DAI score decreased significantly with TAT-GILZ treatment, compared with control (TAT and DSS) and DEX-treated groups. TAT-GILZ treatment reduced the colon weight/length ratio significantly compared with controls, similar to DEX group (Figure 1B,C). Hematoxylin and eosin (H&E) staining of distal colons was analyzed to assess histological damage and infiltration rate. Epithelial damage and crypt loss, as well as leukocyte infiltration, were observed in DSS control, TAT and DEX-treated mice, whereas these parameters were significantly decreased following TAT-GILZ treatment (Figure 1D).

3.2 | TAT-GILZ treatment increases IFNγ levels

Since GILZ can control T cell functions, we investigated the effects of TAT-GILZ treatment on the immune cell environment.[15,23–29] To this end, we first analyzed transcription factors and cytokines that identify specific T cell subpopulations in colon extracts on the day of sacrifice. As shown in Figure 2A, while TAT-GILZ non-significantly upregulated the Th1 transcription factor Tbx21, interestingly increased IFNγ levels significantly if compared to TAT and the DEX group. Th2 and Th17 cells were not affected by TAT-GILZ treatment, whereas the Treg specific transcription factor FoxP3 was upregulated by TAT-GILZ and unexpectedly, also by TAT. So we conclude that TAT-GILZ does not affect FoxP3 expression, since the effects of TAT-GILZ treatment are quite similar to those induced by TAT, but different from control. The cytokines TNFα, IL-6, and IL-1β are typically upregulated during colitis, but these were not affected by TAT-GILZ administration, and they were downregulated by DEX, as expected (Figure 2B).

3.3 | TAT-GILZ treatment improves colon permeability

Next, we investigated the effect of TAT-GILZ treatment on epithelial permeability, one of the most important pathogenic alterations during colitis. Specifically, we performed a FITC-dextran permeability assay. On the day of sacrifice, 4 h after administration of FITC-dextran, blood samples were collected and sera were used to determine the plasmatic FITC-dextran concentration. As shown in Figure 3A, TAT-GILZ treatment reduced permeability significantly versus both control and DEX-treated groups, which conversely showed an increase in colon permeability. Interestingly, the permeability value in the group treated with TAT-GILZ decreased close to the level of the non-colitic group.

3.4 | TAT-GILZ treatment affects zonula occludens-1 expression

In order to search for possible players in permeability controlled by GILZ, we examined the expression of zonula occludens-1 (ZO-1), the most important scaffolding protein that plays a pivotal role in the formation of tight junctions within intestinal epithelial cells. At the time of sacrifice, analysis of ZO-1 mRNA expression levels in colon extracts revealed a downregulation in all colitic groups except for the TAT-GILZ group, in which the level of ZO-1 expression was very similar to that measured in non-colitic mice (Figure 3B). To confirm the mRNA data, we quantified the expression levels of ZO-1 by immunohistochemistry analysis. ZO-1 was downregulated in all groups but increased to levels similar to those of non-colitic mice following TAT-GILZ treatment (Figure 3C). We also analyzed the expression of another important tight junction protein, Claudin-2, which forms paracellular cation and water permeable channels, but no differences were observed across all groups, and DEX only slightly but not significantly suppressed Claudin-2 expression (data not shown), consistent with previous reports.[15,30,31]

3.5 | TAT-GILZ prevents CD74/CD44 complex downregulation and activates ERK and cyclin D1

Since CD74 has been recently shown to promote epithelial cell regeneration during colitis, thereby contributing to ameliorate gut permeability, we investigated the expression of this protein in total colon extracts by RT-PCR.[32] Interestingly, CD74 levels were similar to those of non-colitic mice in the TAT-GILZ-treated group, whereas in all other groups CD74 expression was reduced (Figure 4A). A second receptor that is part of the CD74 signalling complex is CD44.[33] We analyzed CD44 expression levels and found a similar regulation by TAT-GILZ (Figure 4B). CD74 signalling results in phosphorylation of ERK, hence we explored activation of ERK in the same samples.[32] As shown in Figure 4C, TAT-GILZ treatment significantly increased the ratio of pERK over total ERK, similarly to non-colitic group, whereas low activation levels of ERK were observed in all colitic groups, except for DEX-treated mice. ERK signalling cascade involves the activation of cyclins D, so we analyzed the expression of cyclin D1,

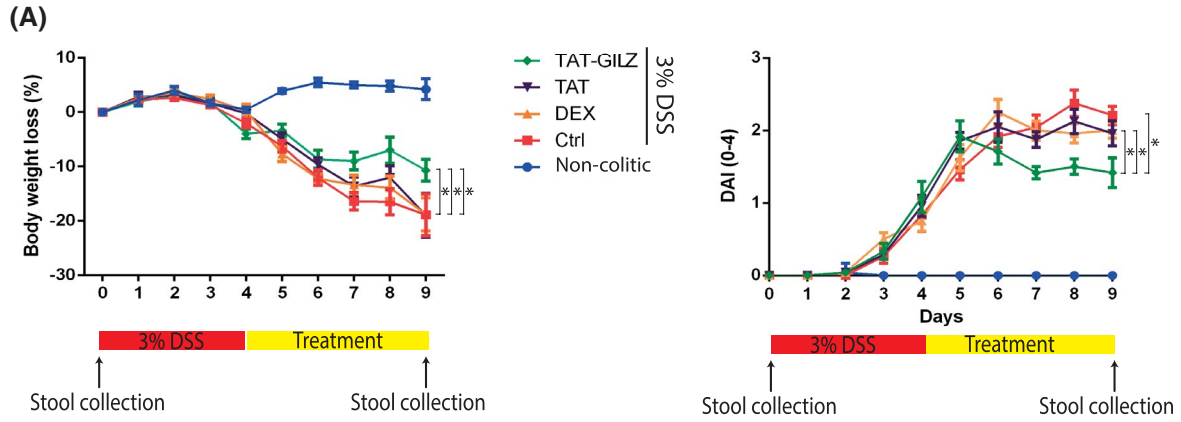

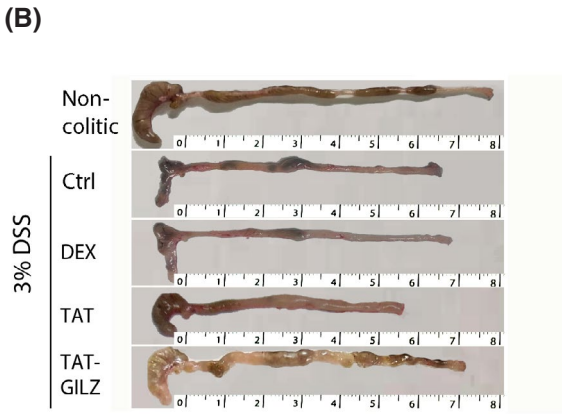

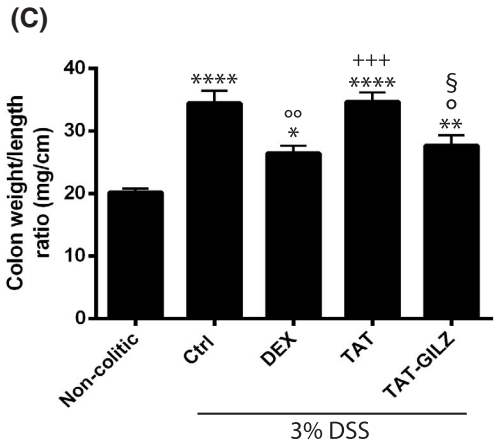

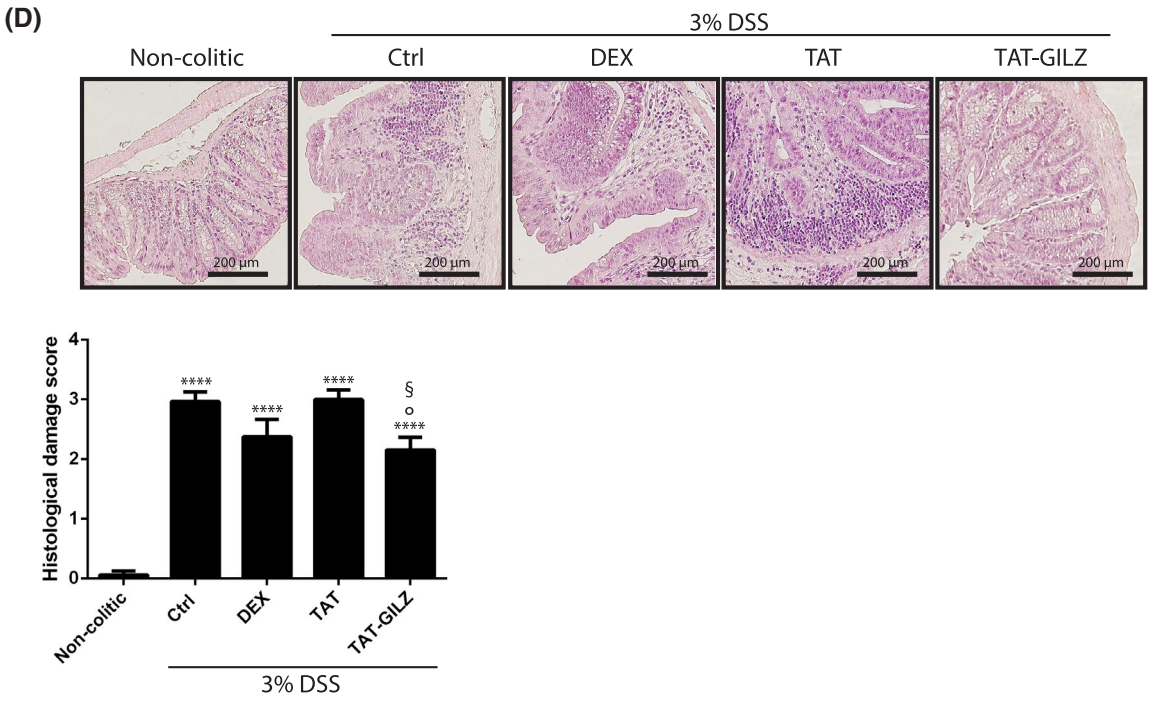

FIGURE 1 Effects of TAT-GILZ treatment in DSS-induced colitis. (A) Mice were exposed to 3% DSS for 4 days, with the exception of one group (non-colitic). Mice received daily the indicated treatments for the subsequent 5 days. Body weight loss and clinical score (DAI) are shown ($n = 8$ per group). TAT-GILZ *$p < .05$ versus TAT, Ctrl and DEX. (B and C) Representative colons for each group and mean weight/length ratio values. (D) Representative H&E stained images for each group and relative histology score. Values are expressed as means ± standard error mean (SEM). $n = 8$. *$p < .05$, **$p < .01$, ****$p < .0001$ versus non-colitic; °$p < .05$ versus Ctrl mice; $^{§}p < .05$ versus TAT group; $^{+}p < .05$ versus DEX-treated mice

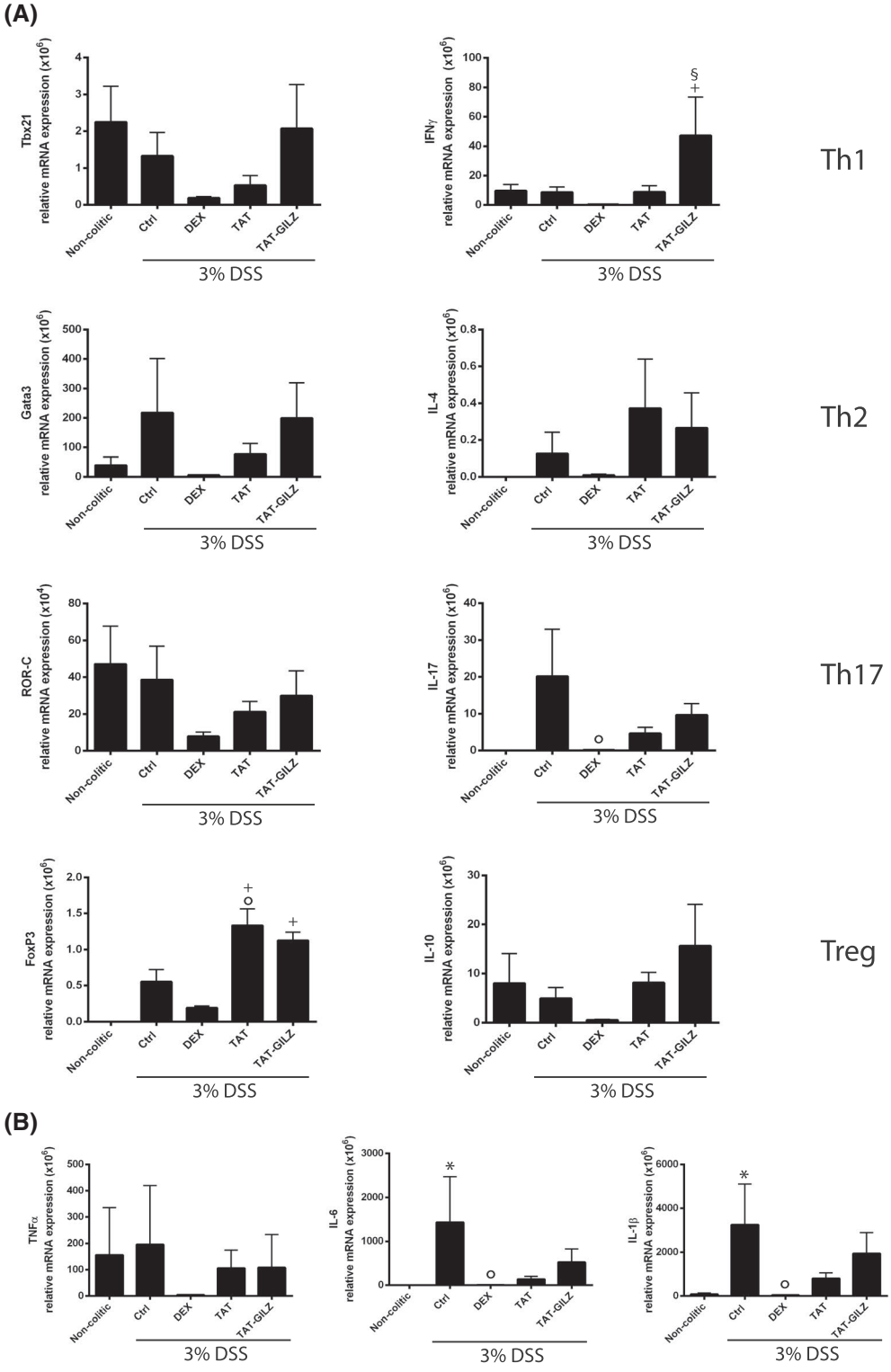

FIGURE 2 Analysis of T cell subtypes and cytokine expression in colon extracts of non-colitic and colitic treated mice, assessed by qRT-PCR. (A and B) Typical transcription factors and cytokines identifying $CD4^+$ Th-specific subtypes and pro-inflammatory cytokines of colitis were evaluated in colon extracts at day 9. Values are expressed as means ± SEM. $n = 8$. *$p < .05$ versus non-colitic; °$p < .05$ versus Ctrl mice; §$p < .05$ versus TAT group; $^+p < .05$ versus DEX-treated mice

D2, and D3.[34] TAT-GILZ treatment increased only cyclin D1 but was ineffective on cyclin D2 and D3 (Figure 4D). Additionally, since GILZ affects the MAPK pathway and NF-κB, we investigated activation of other members such as AKT, p38, and NF-κB, but none were differently modified by TAT-GILZ treatment (not shown).[29,35–38]

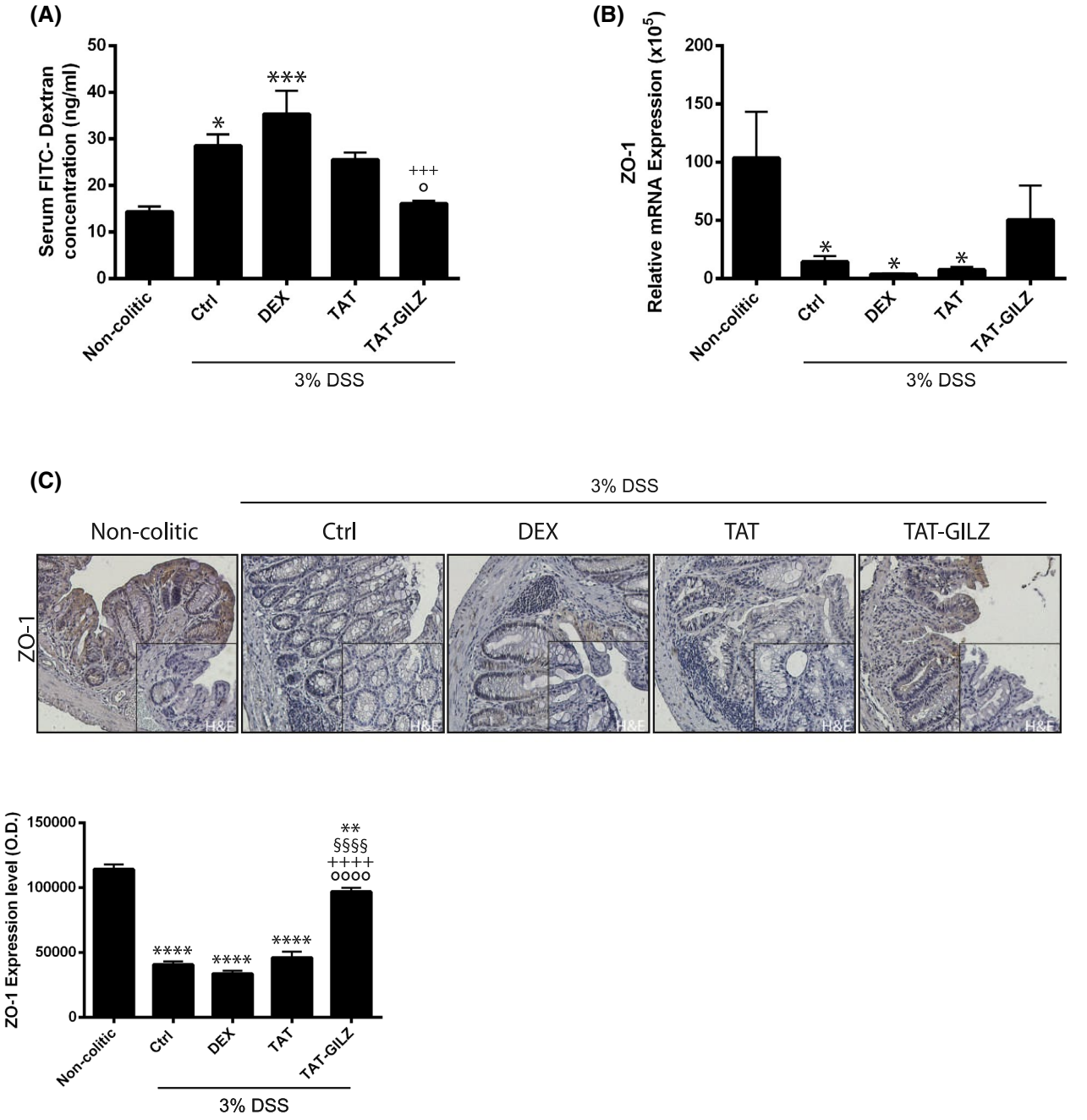

FIGURE 3 Colonic permeability. (A) FITC-dextran permeability assay at day of sacrifice ($n = 4$). (B and C) qRT-PCR ($n = 8$) and immunohistochemistry ($n = 3$) analyses of ZO-1 expression in colon extracts and distal colon sections, respectively. Values are expressed as means ± SEM. $^{*}p < .05$, $^{**}p < .01$, $^{***}p < .001$, $^{****}p < .0001$ versus non-colitic; $^{\circ}p < .05$, $^{\circ\circ\circ\circ}p < .00$ versus Ctrl mice; $^{+++}p < .001$, $^{++++}p < .0001$ versus DEX-treated mice; $^{\S\S\S\S}p < .0001$ versus TAT group

3.6 | TAT-GILZ restores gut dysbiosis

To determine the effects of TAT-GILZ treatment on the gut microbiota, we analyzed the composition of colon microbiota. Intestinal inflammation affected the gut microbiota composition, with the greatest differences in the phyla *Firmicutes*, *Bacteroidetes*, and *Proteobacteria* when control colitic and non-colitic groups were compared (Figure 5A). Interestingly, in the TAT-GILZ-treated group, these phyla were restored to proportions similar to those observed in non-colitic mice (Figure 5A). Additionally, we observed significant changes in the proportion of sequences of different bacterial classes and orders. Specifically, five classes (*Mollicutes*, *Bacteroidia*, *Bacilli*, *Clostridia*, and *Verrumicrobiae*) showed significant differences in DSS colitic mice when compared with non-colitic controls (Figure 5B). *Clostridia*, *Mollicutes*, and *Bacilli* are bacterial members of *Firmicutes* phylum.

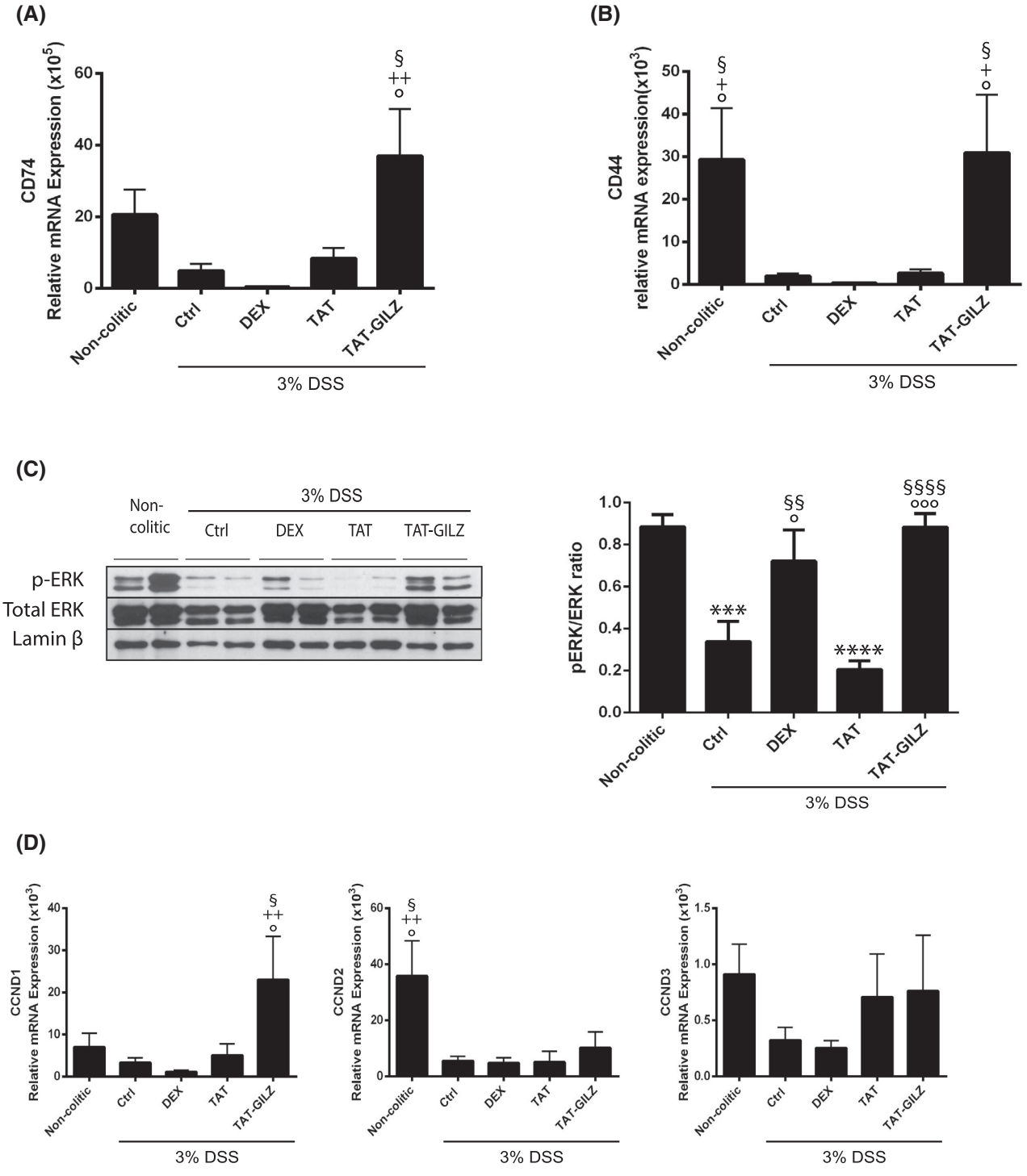

FIGURE 4 Analysis of CD74 complex expression and ERK-derived signalling pathway in colon extracts. (A) qRT-PCR analysis of CD74 expression in non-colitic and treated groups ($n = 8$). (B) qRT-PCR analysis of CD44 expression in non-colitic and treated groups ($n = 8$). (C) Western blotting of ERK phosphorylation (two representative mice per group, $n = 6$). Densitometric analysis refers to eight mice per group. (D) qRT-PCR analysis of cyclins D1, D2, and D3. Values are expressed as means ± SEM. $^{***}p < .001$, $^{****}p < .0001$ versus non-colitic; $^{\circ}p < .05$, $^{\circ\circ\circ}p < .001$ versus Ctrl mice; $^{++}p < .01$ versus DEX-treated mice; $^{\S}p < .05$, $^{\S\S}p < .01$, $^{\S\S\S\S}p < .0001$ versus TAT group

Among them, *Mollicutes* and *Bacilli* populations were increased, whereas *Clostridia* abundance was reduced compared with colitic and non-colitic control mice (Figure 5B). The TAT-GILZ treated group re-established the abundance of *Bacilli* and *Clostridia*, but it was not able to restore the *Mollicutes* population to the level of non-colitic control group (Figure 5B). *Bacteroidia* is a bacterial class belonging to the *Bacteroidetes* phylum, and this class was significantly reduced in colitic mice compared with the non-colitic group. TAT-GILZ treatment increased the

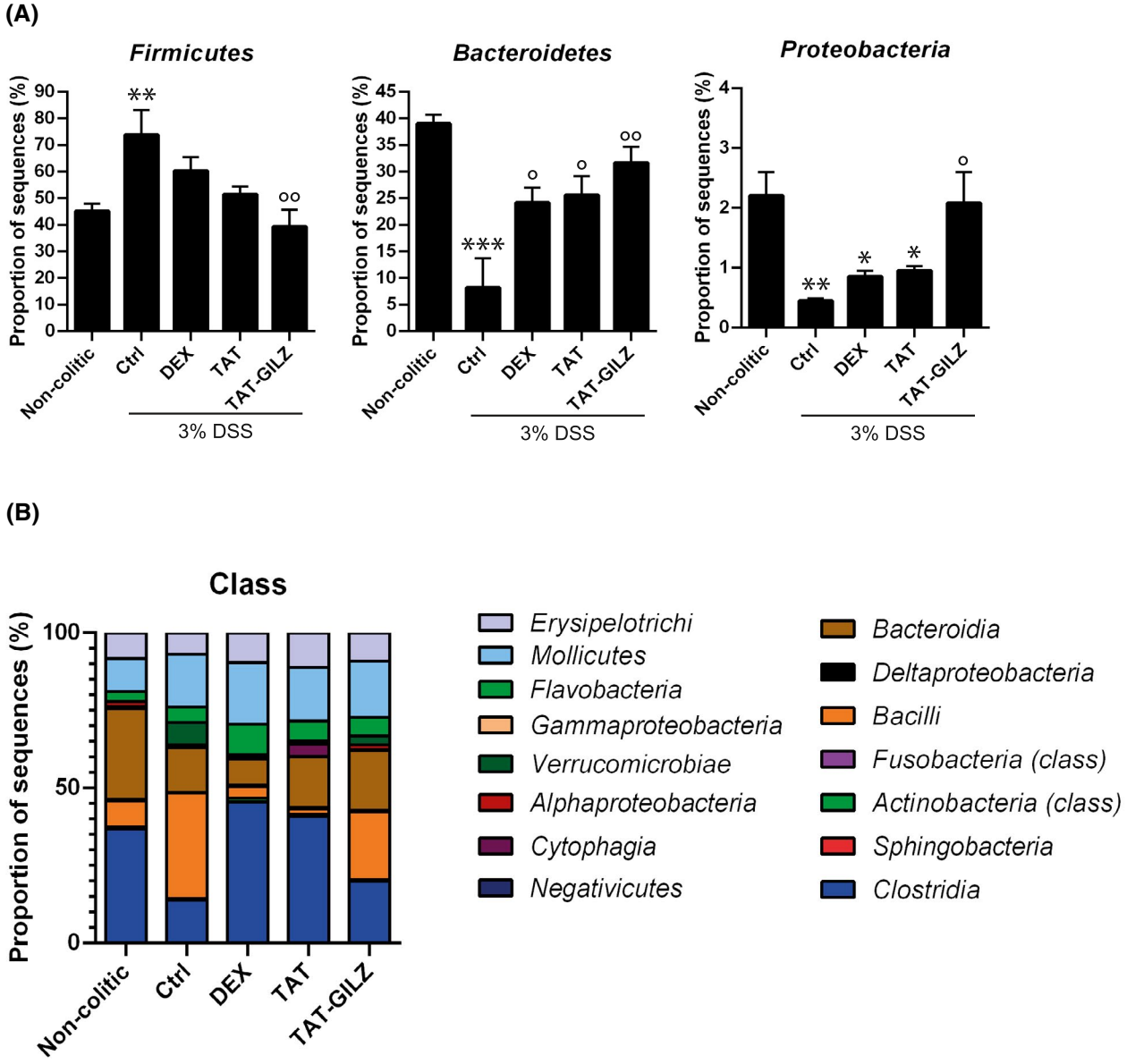

FIGURE 5 Effect of DSS-colitis treatments on (A) bacterial community at phylum level, and (B) bacterial composition at class level. Values are expressed as means ± SEM. $n = 8$. *$p < .05$, **$p < .01$, ***$p < .001$ versus non-colitic; °$p < .05$, °°$p < .01$ versus Ctrl mice

proportion of sequences of this bacterial class (Figure 5B). Moreover, the *Verrumicrobiae* class was significantly increased in the control colitic group, compared with the non-colitic group (Figure 5B), and administration of TAT-GILZ to colitic mice reversed this increase, albeit without statistical differences compared to the colitic group (Figure 5B). When the microbial diversity indices were also determined, significant reductions in microbial species richness (Chao1) and diversity (Shannon) were observed in DSS-treated colitis mice compared with non-colitic mice (Figure 6A). However, TAT-GILZ treatment resulted in a significantly higher diversity index compared with the DSS group (Figure 6A). The community structure of the microbiota was also analyzed using principal coordinate analysis (PCoA). Based on the PCoA plot, there was a clear demarcation between bacterial assemblages from non-colitic and colitic control groups (Figure 6B). The PCA plot showed that the communities in TAT-GILZ-treated colitic mice clearly differed from those in control colitic mice, and were more similar to the non-colitic group (Figure 6B).

4 | DISCUSSION

GILZ exerts anti-inflammatory effects in several mouse models of autoimmune and inflammatory diseases, hence it has been used as a protein-based pharmacological tool

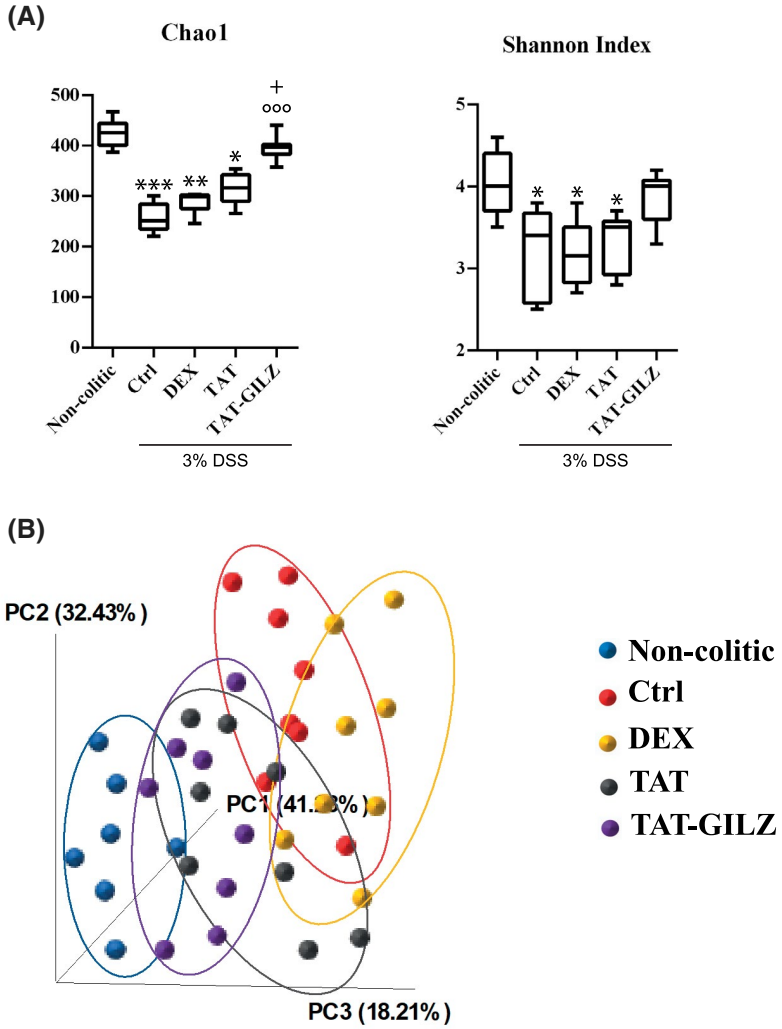

FIGURE 6 Effect of DSS-colitis treatments on (A) microbiome diversity (Chao1 and Shannon index), (B) Beta-diversity by principal coordinate analysis score plot. Data are expressed as means ± SEM. $n = 8$. $^{*}p < .05$, $^{**}p < .01$, $^{***}p < .001$ versus non-colitic; $^{°°°}p < .001$ versus Ctrl mice; $^{+}p < .05$ versus DEX-treated mice

in preclinical studies of IBD, EAE and other diseases, and it is considered an efficacious therapeutic agent.[11,18,39,40] To determine the efficacy of treatment with recombinant TAT-GILZ protein in our model of DSS-induced colitis, we administered TAT-GILZ protein soon after the onset of disease, causing symptoms of overt diarrhoea and significant weight loss. Previous observations demonstrated the efficacy of TAT-GILZ in DNBS-induced colitis when administered at the time of disease induction, thus affecting either Th1 cells or B lymphocytes, depending on the experimental model or the type of transgenic animal used.[13,14] In our model, TAT-GILZ administration was able to ameliorate the disease score for the entire duration of the experiment compared with the other groups, demonstrating, for the first time, that GILZ protein can reduce the colitis-associated symptoms once established. Surprisingly, GILZ-derived effects were different from those induced by DEX. We can reasonably hypothesize that a clear beneficial effect of DEX on weight gain would either require a prolonged treatment duration in our model, or earlier initiation of treatment. Moreover, several and unknown factors influence the glucocorticoid response in IBDs, since some patients either do not respond or show resistance to glucocorticoid treatment.[41,42] However, as observed at the end of the treatment, and as expected at the molecular level, DEX was efficacious in suppressing the pro-inflammatory cytokines IL-6 and IL-1β, as well as Th-specific cytokines, IFNγ, IL-4, IL-17, and IL-10 (Figure 2), albeit non-significantly with the exception of IL-17, thereby improving the underlying inflammatory process in the gut. This tendency and the non-significant difference in DEX-treated animals may reflect an underlying partial recovery from the disease after 5 days of DSS suspension, which was necessary to establish a model of mild colitis. Conversely, GILZ-derived beneficial effects resulted in body weight gain as well as an improved DAI score, but did not affect T-cell subtype-specific markers like Tbx21, GATA3, and ROR-C. Surprisingly, TAT and TAT-GILZ increased the expression of FoxP3 significantly over controls, raising the question whether TAT can elicit some off-target-effects, which will be investigated in future studies. However, such an effect was not observed in any other experiments of this work, thus confirming that TAT-GILZ itself functions differently from TAT control. IFNγ

identifies Th1 cells together with the Tbx21 transcription factor, hence an increase in IFNγ suggests that TAT-GILZ may favour a shift towards Th1 cells, restoring the Th1/Th2 cell balance, which is altered in DSS-induced colitis with Th2-type prevalent cells. Accordingly, IFNγ levels were significantly increased, as well as levels of Tbx21, although not significantly, in TAT-GILZ group compared with TAT control group. Such finding is at odds with the suppression of IFNγ in B cells in another model of colitis, in which the recombinant GILZ protein was administered at the induction of the disease. Experimental conditions were completely different from ours, since B-cell conditional GILZ-KO mice and Th1-type disease model were used.[14] Furthermore, IFNγ levels can change during the development of the experimental disease, making it difficult to detect similarities in the effect of TAT-GILZ protein. Alternatively, we cannot rule out the possibility that the source of IFNγ is in a different cell type, such as NK cells or macrophages. Nevertheless, according to recent findings, IFNγ has been attributed a protective role in promoting inflammation resolution in models of autoimmune diseases including IBDs.[43,44] Additionally, it is well known that the intestinal immune system can establish immune tolerance towards a huge variety of beneficial microorganisms while preserving immune responses against pathogenic microbes. Moreover, the interplay between the microbiota and the immune system is an extensive bidirectional communication. Although most of studies have focused on the ability of the microbiota to modulate the host immune system, it is clear that the host immune system also has a great influence on the composition of the microbiota.[45] Indeed, our current results support this because IFNγ signalling can influence cross-talk between the host and the microbiota, and can modify the microbiota composition.[46–48] However, it is not known whether this is a direct effect of IFNγ on the epithelium. In fact, the intestinal therapeutic effects of TAT-GILZ are associated with the restoration of gut dysbiosis, which could be mediated, at least partially, by the increased expression of IFNγ in the colonic mucosa, thus contributing to improved healing of inflamed intestinal tissue.

Notably, our data demonstrate that not all the effects of GILZ treatment overlapped with those of GCs, as previously demonstrated in other experimental settings.[49–51] GILZ, unlike the GC receptor, cannot directly interact with DNA, but it can heterodimerize with other partner proteins and therefore influence their target genes. Thus, target genes may diverge between GCs and GILZ. In our experimental system, in sharp contrast with DEX treatment, administration of TAT-GILZ protein ameliorated gut permeability, an effect that has not been reported previously. From this point of view, DEX-induced worsening of permeability is in line with previously reported studies in mice, in which DEX treatment increased gut permeability mimicking that of stressed animals, and in adrenalectomized rats, in which stress did not cause any observable increase in gastrointestinal permeability, demonstrating that glucocorticoids can exert deleterious effects during the treatment of colitis.[52–54]

Among distinct effectors controlling gut permeability, ZO-1 is one of the most important proteins characterizing tight junctions, which form an active barrier in intestinal epithelial cells that regulates the transcellular trafficking.[55] Previous studies demonstrated that ZO-1 is downregulated from day 1 after DSS-colitis induction.[56] Our current results showed that, in contrast with all other experimental groups, TAT-GILZ treatment was able to increase ZO-1 expression, thereby ameliorating permeability. Conversely, DEX reduced ZO-1 expression, which represents another distinctive feature of the effects of TAT-GILZ versus DEX. For the first time, we herein demonstrated that TAT-GILZ acts therapeutically to ameliorate gut permeability defects.

Different elements of the gut mucosa clearly contribute to its role as a physical and immunological defence barrier, including the outer mucus layer containing the commensal gut microbiota, antimicrobial proteins and secretory immunoglobulin A molecules, the central single cell layer harboring specialized epithelial cells and the inner *lamina propria*, where innate and adaptive immune cells reside such as T cells, B cells, macrophages and dendritic cells. It has been reported that dysfunction of the intestinal barrier, which leads to an uncontrolled flux of antigens across the intestinal epithelium, may challenge the immune system and affect the host-microbiome balance.[57–59] Although many studies indicate that the microbiome is a key player in the maintenance of both the mechanical epithelial barrier integrity and its functionality, this interaction is complex and bidirectional. Moreover, the intestinal barrier is not a static structure, but is highly dynamic and responsive to both internal and exogenous stimuli.[60] Therefore, a well-organized epithelial barrier and/or an improvement in intestinal barrier function can stimulate a specific composition of potentially beneficial microbiota, and this can be achieved directly through interaction with epithelial cells or indirectly due to its immunomodulatory effect. As a consequence, improvement in gut functionality exerted by TAT-GILZ would provide an optimal environment for colonization of mucosa surface by potentially beneficial bacteria, including bacteria of *Bacteroidetes* and *Proteobacteria* phyla, as well as inhibiting the growth of potentially harmful bacteria, and enhancing their competitive exclusion and/or excretion. However, the exact mechanism by which TAT-GILZ treatment impacts on microbiome remains unknown. The interactions among microbes, diet, host factors, drugs, and cell to cell involve intricate feedbacks, and no single component/pathway

can account for the final outcome. TAT-GILZ could either be effective directly or indirectly both on the immune cells and on the epithelial layer. As a consequence, the microbiome may change in a few days, as described in previous studies in DSS-experimental colitis, thus contributing to the healing process.[61,62]

Since CD74 was recently found to be involved in protecting the host during colitis by promoting epithelial cell regeneration, we analyzed the expression of CD74 in the gut of mice in our experimental model.[32] CD74 was found to be increased by TAT-GILZ administration, in contrast with all other groups including DEX, further supporting a divergent action of exogenous GILZ over DEX. In addition, CD74 downregulation by DEX is new and in line with the increase in gut permeability we observed in our model, further supporting a pivotal role of CD74 in contributing to the control of this important barrier function. We analyzed also the expression of CD44, a surface receptor associated to the signalling complex of CD74.[33] The expression of CD44 was similar to that of CD74, suggesting an overall increase of the entire receptor complex. To strengthen these findings, we explored those intracellular signalling pathways that lead to cell proliferation and previously described to be linked to CD74 functional activity. One of the main players of MAPK pathway is ERK, which has been previously found to be activated downstream of CD74.[32] TAT-GILZ, as well as DEX treatment, was able to significantly restore ERK phosphorylation, directly involved in cell proliferation and regeneration.[63] To further support this result, we analyzed the expression of three important cyclins such as cyclin D1, D2, and D3, which can be activated by ERK phosphorylation.[34] Only Cyclin D1 increased in expression under TAT-GILZ treatment, suggesting that cell proliferation was occurring.[64] The mechanism underlying ZO-1 and CD74 upregulation by TAT-GILZ is still unknown, but it is reasonable to hypothesize a different mechanism from that of endogenous glucocorticoid-induced GILZ protein. For example, pharmacokinetics of TAT-GILZ and endogenous GILZ might be distinct; only GILZ expression variation over time has been investigated previously, revealing GILZ induction by glucocorticoids in the first 2–6 h of treatment, with persistence of expression up to 24 h.[65–68] Data on the half-life of TAT-GILZ has not been reported yet.

The beneficial effects of TAT-GILZ in our model mirror those obtained in other pre-clinical studies. Although in transgenic animals overexpressing GILZ in T cells, oxazolone-induced colitis worsened the symptoms of the disease, in our model, exogenous administration of TAT-GILZ elicited a healing effect, suggesting that distribution of GILZ protein in all cells exerts multiple effects in several cell types, other than immune cells.[13] In the LPS pleurisy model, both TAT-GILZ pre-treatment and post-treatment promoted the resolution of inflammation[18]; in a model of acute kidney injury, TAT-GILZ favored the suppressive phenotypes of neutrophils and T cells, thus contributing to the protection of kidney against damage[69]; in a model of LPS-induced inflammation, administration of a vector carrying the TAT-GILZ gene protected mice from endotoxemia[70]; finally, in a model of DNBS-induced colitis, TAT-GILZ treatment significantly improved disease symptoms.[13,14]

5 | CONCLUSIONS

Our current results further demonstrate the efficacy of TAT-GILZ treatment, adding a piece of knowledge on the mechanism by which GILZ improves the outcome of colitis, which mainly acts on the permeability, ameliorating also gut dysbiosis. Thus, GILZ recombinant protein is an agent that may not only have beneficial effects on colitis, but may act in a manner superior to GCs, thereby circumventing steroid-associated side effects.

ACKNOWLEDGMENTS

This work was supported by a grant from the Italian Ministry of Education, Universities and Research to SR (PRIN 2017B9NCSX), and grants from "Vini di Batasiolo S.p.A.," Junta de Andalucia (CTS 164) and Instituto de Salud Carlos III (PI19/1058; CP19/00191) through funds from the European Union. CIBER-EHD is funded by the Instituto de Salud Carlos III. Marco Gentili was supported by an EMBO short-term fellowship. The authors thank Pilar Utrilla for allowing the start of this work.

DISCLOSURES

The authors declare no conflict of interest.

AUTHOR CONTRIBUTIONS

Julio Galvez, Simona Ronchetti, and Graziella Migliorati designed research. Marco Gentili, Laura Hidalgo-Garcia, and Teresa Vezza performed research, Marco Gentili, Alba Rodriguez-Nogales analyzed data. Erika Ricci contributed new reagents, Simona Ronchetti, Carlo Riccardi, and Julio Galvez wrote the paper.

ORCID

Simona Ronchetti https://orcid.org/0000-0002-5639-4243

REFERENCES

1. Fuss IJ. Is the Th1/Th2 paradigm of immune regulation applicable to IBD? *Inflamm Bowel Dis*. 2008;14(suppl 2):S110-S112.

2. Gui X, Li J, Ueno A, Iacucci M, Qian J, Ghosh S. Histopathological features of inflammatory bowel disease are associated with different CD4$^+$ T cell subsets in colonic mucosal lamina propria. *J Crohns Colitis*. 2018;12:1448-1458.
3. Solitano V, D'Amico F, Fiorino G, Peyrin-Biroulet L, Danese S. Biosimilar switching in inflammatory bowel disease: from evidence to clinical practice. *Expert Rev Clin Immunol*. 2020;16:1-10.
4. Bourchany A, Gilletta De Saint-Joseph C, Breton A, Barreau F, Mas E. Optimization of biologics to reduce treatment failure in inflammatory bowel diseases. *Curr Opin Pharmacol*. 2020;54:51-58.
5. Ronchetti S, Gentili M, Ricci E, Migliorati G, Riccardi C. Glucocorticoid-induced leucine zipper as a druggable target in inflammatory bowel diseases. *Inflamm Bowel Dis*. 2020;26:1017-1025.
6. LeBlanc JF, Wiseman D, Lakatos PL, Bessissow T. Elderly patients with inflammatory bowel disease: updated review of the therapeutic landscape. *World J Gastroenterol*. 2019;25:4158-4171.
7. Windsor JW, Kaplan GG. Evolving epidemiology of IBD. *Curr Gastroenterol Rep*. 2019;21:40.
8. Bereshchenko O, Migliorati G, Bruscoli S, Riccardi C. Glucocorticoid-induced leucine zipper: a novel anti-inflammatory molecule. *Front Pharmacol*. 2019;10:308.
9. Ayyar VS, DuBois DC, Almon RR, Jusko WJ. Mechanistic multi-tissue modeling of glucocorticoid-induced leucine zipper regulation: integrating circadian gene expression with receptor-mediated corticosteroid pharmacodynamics. *J Pharmacol Exp Ther*. 2017;363:45-57.
10. Ronchetti S, Migliorati G, Riccardi C. GILZ as a mediator of the anti-inflammatory effects of glucocorticoids. *Front Endocrinol*. 2015;6:170.
11. Srinivasan M, Janardhanam S. Novel p65 binding glucocorticoid-induced leucine zipper peptide suppresses experimental autoimmune encephalomyelitis. *J Biol Chem*. 2011;286:44799-44810.
12. Gu RP, Lei BY, Jiang C, Xu GZ. Glucocorticoid-induced leucine zipper suppresses ICAM-1 and MCP-1 expression by dephosphorylation of NF-kappa B p65 in retinal endothelial cells. *Invest Ophth Vis Sci*. 2017;58:631-641.
13. Cannarile L, Cuzzocrea S, Santucci L, et al. Glucocorticoid-induced leucine zipper is protective in Th1-mediated models of colitis. *Gastroenterology*. 2009;136:530-541.
14. Bruscoli S, Sorcini D, Flamini S, et al. Glucocorticoid-induced leucine zipper inhibits interferon-gamma production in B cells and suppresses colitis in mice. *Front Immunol*. 2018;9:1720.
15. Bereshchenko O, Coppo M, Bruscoli S, et al. GILZ promotes production of peripherally induced Treg cells and mediates the crosstalk between glucocorticoids and TGF-beta signaling. *Cell Rep*. 2014;7:464-475.
16. Ricci E, Ronchetti S, Pericolini E, et al. Role of the glucocorticoid-induced leucine zipper gene in dexamethasone-induced inhibition of mouse neutrophil migration via control of annexin A1 expression. *FASEB J*. 2017;31:3054-3065.
17. Percie du Sert N, Hurst V, Ahluwalia A, et al. The ARRIVE guidelines 2.0: updated guidelines for reporting animal research. *J Physiol*. 2020;40(9):1769-1777.
18. Vago JP, Tavares LP, Garcia CC, et al. The role and effects of glucocorticoid-induced leucine zipper in the context of inflammation resolution. *J Immunol*. 2015;194:4940-4950.
19. Crowe AR, Yue W. Semi-quantitative determination of protein expression using immunohistochemistry staining and analysis: an integrated protocol. *Bio-Protocol*. 2019;9(24):1-11.
20. Erben U, Loddenkemper C, Doerfel K, et al. A guide to histomorphological evaluation of intestinal inflammation in mouse models. *Int J Clin Exp Pathol*. 2014;7:4557-4576.
21. Rodriguez-Nogales A, Algieri F, Garrido-Mesa J, et al. Differential intestinal anti-inflammatory effects of *Lactobacillus fermentum* and *Lactobacillus salivarius* in DSS mouse colitis: impact on microRNAs expression and microbiota composition. *Mol Nutr Food Res*. 2017;61:1700144.
22. Meyer F, Paarmann D, D'Souza M, et al. The metagenomics RAST server - a public resource for the automatic phylogenetic and functional analysis of metagenomes. *BMC Bioinformatics*. 2008;9:386.
23. Cannarile L, Delfino DV, Adorisio S, Riccardi C, Ayroldi E. Implicating the role of GILZ in glucocorticoid modulation of T-cell activation. *Front Immunol*. 2019;10:1823.
24. Jones SA, Perera DN, Fan H, Russ BE, Harris J, Morand EF. GILZ regulates Th17 responses and restrains IL-17-mediated skin inflammation. *J Autoimmun*. 2015;61:73-80.
25. Esposito E, Bruscoli S, Mazzon E, et al. Glucocorticoid-induced leucine zipper (GILZ) over-expression in T lymphocytes inhibits inflammation and tissue damage in spinal cord injury. *Neurotherapeutics*. 2012;9:210-225.
26. Pozzesi N, Gizzi S, Gori F, et al. IL-2 induces and altered CD4/CD8 ratio of splenic T lymphocytes from transgenic mice overexpressing the glucocorticoid-induced protein GILZ. *J Chemother*. 2007;19:562-569.
27. Cannarile L, Fallarino F, Agostini M, et al. Increased GILZ expression in transgenic mice up-regulates Th-2 lymphokines. *Blood*. 2006;107:1039-1047.
28. Asselin-Labat ML, Biola-Vidamment A, Kerbrat S, Lombes M, Bertoglio J, Pallardy M. FoxO3 mediates antagonistic effects of glucocorticoids and interleukin-2 on glucocorticoid-induced leucine zipper expression. *Mol Endocrinol*. 2005;19:1752-1764.
29. Ayroldi E, Migliorati G, Bruscoli S, et al. Modulation of T-cell activation by the glucocorticoid-induced leucine zipper factor via inhibition of nuclear factor kappaB. *Blood*. 2001;98:743-753.
30. Venugopal S, Anwer S, Szaszi K. Claudin-2: roles beyond permeability functions. *Int J Mol Sci*. 2019;20(22):5655.
31. Fischer A, Gluth M, Weege F, et al. Glucocorticoids regulate barrier function and claudin expression in intestinal epithelial cells via MKP-1. *Am J Physiol Gastrointest Liver Physiol*. 2014;306:G218-G228.
32. Farr L, Ghosh S, Jiang N, et al. CD74 signaling links inflammation to intestinal epithelial cell regeneration and promotes mucosal healing. *Cell Mol Gastroenterol Hepatol*. 2020;10:101-112.
33. Shi X, Leng L, Wang T, et al. CD44 is the signaling component of the macrophage migration inhibitory factor-CD74 receptor complex. *Immunity*. 2006;25:595-606.
34. Torii S, Yamamoto T, Tsuchiya Y, Nishida E. ERK MAP kinase in G cell cycle progression and cancer. *Cancer Sci*. 2006;97:697-702.
35. Wang Q, Guo XL, Wells-Byrum D, Noel G, Pritts TA, Ogle CK. Cytokine-induced epithelial permeability changes are regulated by the activation of the p38 mitogen-activated protein kinase pathway in cultured Caco-2 cells. *Shock*. 2008;29:531-537.
36. Cheng Q, Fan H, Ngo D, et al. GILZ overexpression inhibits endothelial cell adhesive function through regulation of NF-kappaB and MAPK activity. *J Immunol*. 2013;191:424-433.
37. Ricci E, Ronchetti S, Gabrielli E, et al. GILZ restrains neutrophil activation by inhibiting the MAPK pathway. *J Leukoc Biol*. 2019;105:187-194.

38. Joha S, Nugues AL, Hetuin D, et al. GILZ inhibits the mTORC2/AKT pathway in BCR-ABL^{+} cells. *Oncogene*. 2012;31:1419-1430.
39. Vago JP, Galvao I, Negreiros-Lima GL, et al. Glucocorticoid-induced leucine zipper modulates macrophage polarization and apoptotic cell clearance. *Pharmacol Res*. 2020;158:104842.
40. Srinivasan M, Bayon B, Chopra N, Lahiri DK. Novel nuclear factor-KappaB targeting peptide suppresses beta-amyloid induced inflammatory and apoptotic responses in neuronal cells. *PLoS ONE*. 2016;11:e0160314.
41. Farrell RJ, Kelleher D. Glucocorticoid resistance in inflammatory bowel disease. *J Endocrinol*. 2003;178:339-346.
42. Sidoroff M, Kolho KL. Glucocorticoid sensitivity in inflammatory bowel disease. *Ann Med*. 2012;44:578-587.
43. Kominsky DJ, Campbell EL, Ehrentraut SF, et al. IFN-gamma-mediated induction of an apical IL-10 receptor on polarized intestinal epithelia. *J Immunol*. 2014;192:1267-1276.
44. Muzaki AR, Tetlak P, Sheng J, et al. Intestinal CD103^{+}CD11b^{-} dendritic cells restrain colitis via IFN-gamma-induced anti-inflammatory response in epithelial cells. *Mucosal Immunol*. 2016;9:336-351.
45. Kabat AM, Srinivasan N, Maloy KJ. Modulation of immune development and function by intestinal microbiota. *Trends Immunol*. 2014;35:507-517.
46. Brodziak F, Meharg C, Blaut M, Loh G. Differences in mucosal gene expression in the colon of two inbred mouse strains after colonization with commensal gut bacteria. *PLoS ONE*. 2013;8:e72317.
47. Thompson CL, Hofer MJ, Campbell IL, Holmes AJ. Community dynamics in the mouse gut microbiota: a possible role for IRF9-regulated genes in community homeostasis. *PLoS ONE*. 2010;5:e10335.
48. Deriu E, Boxx GM, He X, et al. Influenza virus affects intestinal microbiota and secondary salmonella infection in the gut through type I interferons. *PLoS Pathog*. 2016;12:e1005572.
49. Cheng Q, Morand E, Yang YH. Development of novel treatment strategies for inflammatory diseases-similarities and divergence between glucocorticoids and GILZ. *Front Pharmacol*. 2014;5:169.
50. Zhang W, Yang N, Shi XM. Regulation of mesenchymal stem cell osteogenic differentiation by glucocorticoid-induced leucine zipper (GILZ). *J Biol Chem*. 2008;283:4723-4729.
51. Shi X, Shi W, Li Q, et al. A glucocorticoid-induced leucine-zipper protein, GILZ, inhibits adipogenesis of mesenchymal cells. *EMBO Rep*. 2003;4:374-380.
52. Xu CL, Lee SK, Zhang DC, Frenette PS. The gut microbiome regulates psychological-stress-induced inflammation. *Immunity*. 2020;53:417-428.e4.
53. Zong Y, Zhu S, Zhang S, Zheng G, Wiley JW, Hong S. Chronic stress and intestinal permeability: lubiprostone regulates glucocorticoid receptor-mediated changes in colon epithelial tight junction proteins, barrier function, and visceral pain in the rodent and human. *Neurogastroenterol Motil*. 2019;31:e13477.
54. Meddings JB, Swain MG. Environmental stress-induced gastrointestinal permeability is mediated by endogenous glucocorticoids in the rat. *Gastroenterology*. 2000;119:1019-1028.
55. Nusrat A, Turner JR, Madara JL. Molecular physiology and pathophysiology of tight junctions. IV. Regulation of tight junctions by extracellular stimuli: nutrients, cytokines, and immune cells. *Am J Physiol Gastrointest Liver Physiol*. 2000;279:G851-G857.
56. Poritz LS, Garver KI, Green C, Fitzpatrick L, Ruggiero F, Koltun WA. Loss of the tight junction protein ZO-1 in dextran sulfate sodium induced colitis. *J Surg Res*. 2007;140:12-19.
57. Morgan XC, Tickle TL, Sokol H, et al. Dysfunction of the intestinal microbiome in inflammatory bowel disease and treatment. *Genome Biol*. 2012;13:R79.
58. Zuo T, Ng SC. The Gut microbiota in the pathogenesis and therapeutics of inflammatory bowel disease. *Front Microbiol*. 2018;9:2247.
59. Roy U, Galvez EJC, Iljazovic A, et al. Distinct microbial communities trigger colitis development upon intestinal barrier damage via innate or adaptive immune cells. *Cell Rep*. 2017;21:994-1008.
60. Turner JR. Intestinal mucosal barrier function in health and disease. *Nat Rev Immunol*. 2009;9:799-809.
61. Huang EY, Inoue T, Leone VA, et al. Using corticosteroids to reshape the gut microbiome: implications for inflammatory bowel diseases. *Inflamm Bowel Dis*. 2015;21:963-972.
62. Garrido-Mesa J, Rodriguez-Nogales A, Algieri F, et al. Immunomodulatory tetracyclines shape the intestinal inflammatory response inducing mucosal healing and resolution. *Br J Pharmacol*. 2018;175:4353-4370.
63. Starlets D, Gore Y, Binsky I, et al. Cell-surface CD74 initiates a signaling cascade leading to cell proliferation and survival. *Blood*. 2006;107:4807-4816.
64. Filmus J, Robles AI, Shi W, Wong MJ, Colombo LL, Conti CJ. Induction of cyclin D1 overexpression by activated ras. *Oncogene*. 1994;9:3627-3633.
65. Berrebi D, Bruscoli S, Cohen N, et al. Synthesis of glucocorticoid-induced leucine zipper (GILZ) by macrophages: an anti-inflammatory and immunosuppressive mechanism shared by glucocorticoids and IL-10. *Blood*. 2003;101:729-738.
66. Zimmer A, Luce S, Gaignier F, et al. Identification of a new phenotype of tolerogenic human dendritic cells induced by fungal proteases from *Aspergillus oryzae*. *J Immunol*. 2011;186:3966-3976.
67. Escoll P, Ranz I, Munoz-Anton N, et al. Sustained interleukin-1beta exposure modulates multiple steps in glucocorticoid receptor signaling, promoting split-resistance to the transactivation of prominent anti-inflammatory genes by glucocorticoids. *Mediators Inflamm*. 2015;2015:347965.
68. Espinasse MA, Hajage D, Montravers P, et al. Neutrophil expression of glucocorticoid-induced leucine zipper (GILZ) anti-inflammatory protein is associated with acute respiratory distress syndrome severity. *Ann Intensive Care*. 2016;6:105.
69. Baban B, Marchetti C, Khodadadi H, et al. Glucocorticoid-induced leucine zipper promotes neutrophil and T-cell polarization with protective effects in acute kidney injury. *J Pharmacol Exp Ther*. 2018;367:483-493.
70. Pinheiro I, Dejager L, Petta I, et al. LPS resistance of SPRET/Ei mice is mediated by Gilz, encoded by the Tsc22d3 gene on the X chromosome. *EMBO Mol Med*. 2013;5:456-470.

How to cite this article: Gentili M, Hidalgo-Garcia L, Vezza T, et al. A recombinant glucocorticoid-induced leucine zipper protein ameliorates symptoms of dextran sulfate sodium-induced colitis by improving intestinal permeability. *FASEB J*. 2021;35:e21950. doi:10.1096/fj.202100778RRRR